

مطالعه جذب سطحی L-آلانین، L-تریپتوفان و L-تیروزین از نمونه های آبی با استفاده از نانوذرات مغناطیسی Fe₃O₄ اصلاح شده با مایع یونی

صدیقه کامران

بخش شیمی، دانشگاه پیام نور، صندوق پستی ۳۶۹۷-۱۹۳۹۵، تهران، ایران

تاریخ دریافت: ۷ مرداد ۱۳۹۵ تاریخ پذیرش: ۲۹ مهر ۱۳۹۵

Study of the Adsorption of L-Phenylalanine, L-Tryptophan, and L-Tyrosine from Aqueous Samples by Fe₃O₄ Modified Magnetic Nanoparticles with Ionic Liquid

Sedigheh Kamran

Department of Chemistry, Payame Noor University, P.O. Box 19395-4697 Tehran, Iran

Received: 28 July 2016

Accepted: 20 October 2016

چکیده

ما نانوذراتی از نوع Fe₃O₄ ترکیب دوتایی آن با مایع یونی ۱-اکتیل-۳-متیل ایمیدازولیوم برمید را تهیه و شناسایی کردیم و در جذب آلانین، تریپتوفان و تیروزین مورد استفاده قرار گرفت. اندازه ذرات میانگین و مورفولوژی سطح نانوذرات با تکنیک های FTIR، XRD و TEM بررسی شد. pH نقطه بار صفر هر دو نانوذرات و نانوذرات ترکیب شده با مایع یونی بدست آمد. نتایج آزمایشی تحت شرایط بهینه زیر بدست آمد: مقدار نانوذره ۰/۱۵ گرم و زمان های پاسخ ۵، ۱۰ و ۱۵ دقیقه به ترتیب برای تریپتوفان، تیروزین و فنیل آلانین در غلظت اولیه ۵/۰×۱۰^{-۴} مولار از آمینو اسید. ارزیابی های ایزوترم نشان می دهد مدل فروندلیچ نسبت به مدل داینین-رادوشکوویچ با داده های تجربی تطابق بیشتری دارد. ماکزیم ظرفیت جذب برای تریپتوفان، تیروزین و فنیل آلانین عبارتست از: ۱۲/۷۴۰، ۳/۵۵ و ۳۵/۶۲ میلی گرم بر گرم جاذب. فرآیند جذب گرماگیر می باشد. هر دو فنیل آلانین و تیروزین امکان واجذب شدنشان از جاذب به وسیله محلول های ۱/۰ و ۲/۰ مولار NaOH وجود دارد. همچنین تریپتوفان بطور کامل در حضور محلولی از ۱/۰ مولار NaCl و ۱/۰ مولار NaOH از جاذب واجذب می شود. بنابراین نانوذرات قابلیت دوباره استفاده شدن را دارند.

واژه های کلیدی

نانوذرات مغناطیسی؛ جذب سطحی؛ آمینواسیدها.

Abstract

Fe₃O₄ nanoparticles and their binary mixtures ([C₈MIM]-Fe₃O₄) with 1-Octyl-3-methylimidazolium bromide were prepared and characterized as ionic liquid for using in the adsorption of phenylalanine, tryptophan, and tyrosine. The characteristics of [C₈MIM]-Fe₃O₄ nanoparticles were investigated via using TEM, XRD and FTIR techniques. The pH of the point of zero charge (pH_{pzc}) of both Fe₃O₄ and [C₈MIM]-Fe₃O₄ were obtained based on the experimental curves corresponding to the immersion technique. Experimental results were obtained under optimum operational conditions of: nanoparticle amount of 0.015 g and a contact times of 5, 10, 15 minutes for tryptophan (Trp), tyrosine (Tyr) and phenylalanine (Phe), respectively, when initial concentration of each amino acid was 5.0×10⁻⁴ mol L⁻¹. The isotherm evaluations revealed that the Freundlich model attained better fits to the equilibrium data than the Dubinin-Radushkevich model. The maximum obtained adsorption capacities of Tyr, Trp and Phe were 12.74, 3.55 and 35.62 mg amino acid per gram of adsorbent, respectively. The applicability of pseudo-first order and pseudo-second order kinetic models was estimated on the basis of comparative analysis of the corresponding rate parameters, equilibrium adsorption capacity and correlation coefficients. Furthermore, the adsorption processes were found endothermic. Both phenylalanine and tyrosine were desorbed from [C₈MIM]-Fe₃O₄ nanoparticles by using NaOH aqueous solution with concentrations of 1.0 and 2.0 mol L⁻¹, respectively. Tryptophan was completely desorbed in the presence of a mixture of 1.0 mol L⁻¹ NaCl and 1.0 mol L⁻¹ NaOH. The nanoparticles thus were recycled.

Keywords

Magnetic Nanoparticle; Ionic Liquid; Adsorption; Amino Acids

1. INTRODUCTION

Amino acids make a significant class of bioorganic compounds mainly because they

constitute the building blocks of proteins. They are widely used in food industry as nutritional supplements and as quality-improving agents for

proteins [1,2]. Additionally, amino acids are used as building blocks for production of agrochemical and pharmaceutical compounds and also can be applied in synthesise of oligopeptides or other larger size biomolecules. They have also found applications in such areas as the biodegradable plastics industry [3], drug delivery systems [4] or in stereoselective laboratory synthesis [5]. Amino acids contain carboxyl and amino functional groups which are responsible for their adsorption ability [6].

Amongst the 20 common amino acids which biochemically build proteins and perform specific functions in the human body, nine are classified as essential, due to the inability of the human body in their synthesise [7]. In the past, the technology for the production of amino acids was largely based on recovery from protein hydrolysates; today fermentation with genetically engineered bacterial strains constitutes the main production route [8]. Several steps are, in general, required in order to recover and purify the amino acids from fermentation broths. Ion exchange is one of the processes that is commonly used for separation of amino acids both on analytical and industrial scales. To improve the efficiency of recovery, several techniques for separation and purification of amino acids from wastewaters, coming from fermentations broths, have been employed [9-10]. In this regard, partitioning of amino acids into various phases including ionic liquids and reverse micelles has also been studied [11,12].

Many studies have been reported for adsorption of amino acids on various adsorbing materials including activated carbon, silica, ion exchangers, alumina, zeolites, and polymeric resins [13-18]. Adsorptive separations are widely used in chemical engineering applications for the purification of fluid streams, recovery of solutes and bulk separations. The importance of adsorption processes has been recently stressed in various reviews [19-21].

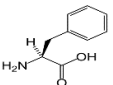
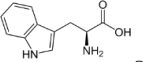
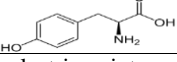
These above applications usually require amino acids to be adsorbed in the form of well-ordered layers onto a solid surface. Understanding the mechanism by which amino acids adsorb onto an

inorganic surface is an important concern in treatment of bioproducts and in various biotechnological fields, such as the preparation of biocompatible materials and biosensors [22].

Room temperature ionic liquids (RTILs) as useful environment friendly green solvents, have recently attracted special attentions due to their unique physical and chemical properties such as nonvolatile, non-flammable, excellent solvation qualities and high thermal stability [23]. Since RTILs can dissolve many different organic, organometallic and inorganic compounds, they are applied in many fields of analytical chemistry. Ionic liquid-based extraction has some disadvantages such as low rate of mass transfer, long equilibrium time, difficulty in separate -phase and entraining loss of IL to aqueous phase [24]. These limitations can be overcome by modification of solid phase with ionic liquids. Some studies have been recently focused on the application of RTILs from extraction or adsorption of biomolecules, metal ions and polycyclic aromatic hydrocarbons [25-27]. However, the application of supported ionic liquid phase for the adsorption of amino acids has not been reported.

The present study focuses on characterization of the adsorption processes of phenylalanine, tryptophan and tyrosine (Table 1) on the surface of magnetic nanoparticles of Fe₃O₄ modified by ionic liquid, [C8MIM][Br]. The results might be useful because adsorption and separation of biomolecules including amino acids are important due to their potential applications in many frontiers of modern materials science including biocatalysis, biosensing, drug release and separation of biomolecules [28]. In this regard, electron microscopy (TEM), X-ray diffraction (XRD), and Fourier transform infrared (FTIR) spectroscopy have been utilized for this characterization. Adsorption isotherms, kinetic of adsorption and thermodynamic parameters are also characterized and reported. To the best of our knowledge, adsorption of these amino acids on Fe₃O₄ magnetic nanoparticles modified by ionic liquids has not been reported.

Table 1. Chemical structure of the amino acids and their dissociation constants at 25 °C.

Amino acid	Chemical structure	Carboxylic acid pK _a	Ammonium pK _a	Pk _a PhOH	pI ^a	Volume (Å ³)	Hydrophobicity index
Phenylalanine		1.83	9.13		5.48	189.9	1.0
Tryptophan		2.38	9.39		5.89	227.8	0.878
Tyrosine		2.2	9.11	10.07	5.66	193.6	0.88

^a pI is the pH of isoelectric point.

2. EXPERIMENTAL

2.1. Apparatus

A double beam UV-visible Shimadzu spectrophotometer Model 1601 equipped with a 1-cm quartz cell was used for recording the visible spectra and absorbance measurements. The FTIR spectra were recorded on a Shimadzu FTIR 8000 spectrometer. The XRD measurements were performed on the XRD Bruker D8 Advance. A transmission electron microscope (Philips CM 10 TEM) was used for recording the TEM images. A Metrohm 780 pH meter was used for monitoring the pH values. A water Ultrasonicator (Model CD-4800, China) was used to disperse the nanoparticles in solution and a super magnet Nd-Fe-B (1.47 T, 10×5×2 cm) was used. All measurements were performed at ambient temperature.

2.2. Chemicals and reagents

All chemicals and reagents were of analytical grades. Phenylalanine, tryptophan, and tyrosine, 1-bromooctane, 1-methylimidazolium, sodium hydroxide, hydrochloric acid (37% w/w), sodium chloride, FeCl₃·6H₂O (96 % w/w) and FeSO₄·7H₂O (99.9 % w/w) were purchased from Merck. The amino acids solutions with concentrations in the range of 0.020-1.0 mg mL⁻¹ were prepared by successive dilution of their fresh stock solutions (1.0 mg mL⁻¹) with distilled water. The pH adjustments were performed with HCl and NaOH solutions (0.01-1.0 mol L⁻¹). The ionic liquid 1-octyl-3-methylimidazolium bromide, [C₈MIM][Br], was prepared according to the same procedure reported for 1-butyl-3-methylimidazolium bromide in the literature; only 1-bromooctane was used instead of 1-bromobutane [29].

2.3. Fabrication of ionic liquid-modified magnetic nanoparticles

The nanoparticles of Fe₃O₄ were synthesized by mixing ferrous sulfate and ferric chloride in NaOH solution with constant stirring as recommended [30]. To obtain maximum yield for magnetic nanoparticles during co-precipitation process, the ideal molar ratio of Fe²⁺/Fe³⁺ was about 0.5. The precipitates were heated at 80 °C for 30 minutes and were sonicated for 20 minutes, then washed three times with 50 mL distilled water each time.

Modification of Fe₃O₄ nanoparticles was carried out using ionic liquid [C₈MIM][Br] under vigorous magnetic stirring for 30 minutes at 50 °C. The modified iron oxide nanoparticles ([C₈MIM]-Fe₃O₄) were collected by applying a magnetic field with an intensity of 1.4 T. The [C₈MIM]-Fe₃O₄ nanoparticles were washed three

times with 50 mL distilled water each time. Nanoparticles and distilled water mixture was dispersed by ultrasonicator for 10 minutes at room temperature. Then, the [C₈MIM]-Fe₃O₄ nanoparticles were magnetically separated [31].

2.4. Adsorption equilibrium of amino acids

Adsorption of amino acids onto [C₈MIM]-Fe₃O₄ nanoparticles from aqueous solutions was investigated batch-wise. The magnetic nanoparticles (0.015 g) were incubated with 20 mL of the aqueous solutions of amino acids for 1-16 minutes (equilibrium time) in a beaker agitated magnetically. After mixing, magnet was removed and washed with distilled water. Then, the adsorbed amino acids on the surface of [C₈MIM]-Fe₃O₄ nanoparticles was magnetically separated and the mother solution was analyzed spectrophotometrically for the residual of phenylalanine, tryptophan, and tyrosine at 263, 279.5, 275 nm, respectively.

Effects of amino acids concentration, pH of the aqueous solution, temperature, and ionic strength on the adsorption capacity of the adsorbent were studied. To determine the effect of pH on the adsorption, pH of the solution was changed in the range of 3.0-11.0. To observe the effects of the initial concentration of amino acids on their adsorption, the concentration of each amino acid was tested from 0.020 to 1.0 mg mL⁻¹. To observe the effects of temperature on the adsorption, adsorption studies were carried out in the temperature range of 5 to 35 °C.

To study the adsorption kinetics of an amino acid, the modified Fe₃O₄ (0.015 g) was incubated with 10 ml of the buffer solutions (at a specific pH), containing 20 mg L⁻¹ of amino acid, and the suspension was immediately stirred for different periods of time. Adsorption kinetic data were obtained by measuring the concentration of amino acid in the solution at different times after removing the magnetic nanoparticles.

The equilibrium binding amount of the amino acid adsorbed onto [C₈MIM]-Fe₃O₄ was calculated according to the following equation:

$$q_e = \frac{V(C_0 - C_e)}{m} \quad (1)$$

where q_e (in mg g⁻¹) is the adsorption capacity (mg) amino acid adsorbed onto gram amount of [C₈MIM]-Fe₃O₄, V is the volume of the amino acid solution (in liter), C_0 and C_e are the initial and equilibrium amino acid concentrations (in mg L⁻¹), respectively, and m is the mass (in gram) of dry [C₈MIM]-Fe₃O₄ added.

3. RESULT AND DISCUSSION

3.1. Characterization of Fe_3O_4 and $[C_8MIM]-Fe_3O_4$

The peaks positions and relative intensities observed in XRD patterns of both $[C_8MIM]-Fe_3O_4$ nanoparticles and standard Fe_3O_4 are shown in Fig. 1 for comparison. Five characteristics peaks for both Fe_3O_4 and $[C_8MIM]-Fe_3O_4$ corresponding to indices (220), (311), (400), (511), and (440) are observed. Although the magnetic nanoparticle surfaces in $[C_8MIM]-Fe_3O_4$ was coated with ionic liquid, analysis of XRD patterns of both Fe_3O_4 and $[C_8MIM]-Fe_3O_4$ indicated very distinguishable peaks for magnetite crystal, which means that these particles have phase stability [32-33].

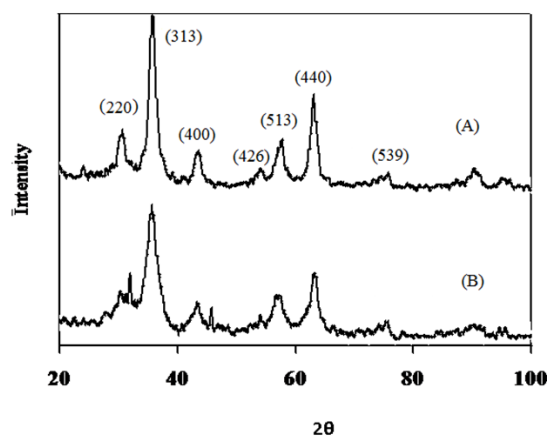


Fig. 1. XRD pattern of Fe_3O_4 , A; and $[C_8MIM]-Fe_3O_4$, B.

The FTIR spectra of Fe_3O_4 , ionic liquid and $[C_8MIM]-Fe_3O_4$ are shown in Fig. 2. In the case of Fe_3O_4 , the broad absorption band at 3440 cm^{-1} shows the presence of surface hydroxyl groups (O–H stretching). The bands at low wave numbers ($\leq 700\text{ cm}^{-1}$) relate to vibration of Fe–O bonds in magnetite. The presence of magnetite nanoparticles can be demonstrated by appearance of two strong absorption bands around 585 cm^{-1} [34,35]. The Fe–O bond peak of the bulk magnetite is observed at 570.9 cm^{-1} . In the spectrum of ionic liquid (Fig. 2-B), a longer hydrocarbon chain in $[C_8MIM][Br]$ gives significantly stronger peaks in the ranges of 2800–3100 and 1465–1640 cm^{-1} . In the FTIR spectrum of $[C_8MIM]-Fe_3O_4$, the significant absorption band at 2931.6 cm^{-1} is due to the C–H stretching. The peak which is observed around 1180 cm^{-1} corresponding to the in-plane C–H deformation vibration of imidazolium ring (Fig. 2-B). The absorption band at 1458.1 cm^{-1} indicates the presence of C–N stretching. The absorption band at 1627.8 cm^{-1} is related to the hetro-aromatic C–H bond stretching.

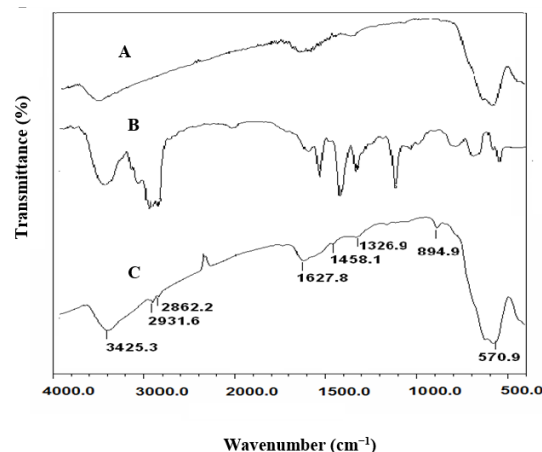


Fig. 2. FTIR spectra of Fe_3O_4 , A; IL, B; and $[C_8MIM]-Fe_3O_4$, C.

The TEM image of Fe_3O_4 nanoparticles, Fig. 3, indicated that the average diameter of Fe_3O_4 nanoparticles was about $\sim 10\text{ nm}$ and that of $[C_8MIM]-Fe_3O_4$ was $\sim 13\text{ nm}$. If it is assumed that the difference of 3 nm in the mean sizes of both nanoparticles is significant, then it revealed that ionic liquid caused agglomeration of Fe_3O_4 nanoparticles which was expected as ionic liquids could reduce the surface charges of nanoparticles. This case is similar to what can be observed for colloidal particles when an inert electrolyte is added to their aqueous solutions.

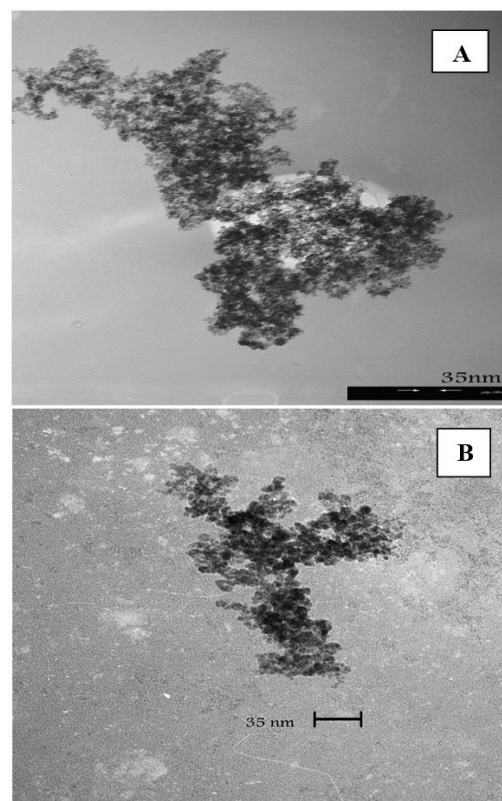


Fig. 3. The TEM image of Fe_3O_4 , A; and $[C_8MIM]-Fe_3O_4$, B.

The experimental curves corresponding to the immersion technique [36] were obtained for both sorbents and are presented in Fig. 4. Suspensions of 5.5 g L^{-1} of sorbents were prepared and individually were brought into contact with 0.10 mol L^{-1} of NaCl solutions adjusted at different pH values. The aqueous suspensions were agitated for 48 hours until the equilibrium pH was achieved. The pH value at the point of zero charge (pH_{pzc}) was determined by plotting the difference of final and initial pHs (ΔpH) versus the initial pH. As it is shown in Fig. 4, the pH_{pzc} values of both Fe_3O_4 and $[\text{C}_8\text{MIM}]\text{-Fe}_3\text{O}_4$ are 6.5 and 8.0, respectively, meaning that the pH of Fe_3O_4 has shifted from 6.5 to 8.0 after being modified with ionic liquid. This observation confirmed the deposition of ionic liquid onto the surface of Fe_3O_4 and it also revealed that $[\text{C}_8\text{MIM}]\text{-Fe}_3\text{O}_4$ was positively charged at $\text{pH} < 8.0$. It is noticeable that pH_{pzc} value for Fe_3O_4 is corresponding to the reported value in the literature [37]. The data points obtained in this figure and the following figures are mostly the average of two measurements.

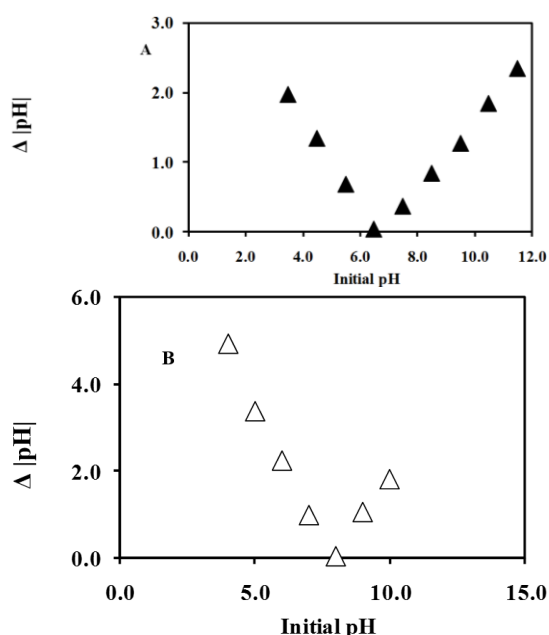


Fig. 4. Immersion technique curves of Fe_3O_4 , A; and $[\text{C}_8\text{MIM}]\text{-Fe}_3\text{O}_4$, B.

3.2. Adsorption of amino acids from aqueous solutions

3.2.1. Effect of initial pH

The effect of the initial pH of the sample solution on the adsorption of phenylalanine, tryptophan, and tyrosine onto $[\text{C}_8\text{MIM}]\text{-Fe}_3\text{O}_4$ surface was assessed at different pH values ranging from 3.0 to 11.0. The initial concentrations of phenylalanine, tryptophan, and tyrosine and adsorbent amount were set at 100 mg L^{-1} and

0.015 g , respectively. Each solution was stirred for a period of 10 minutes while the experiments were performed in batch technique. The results are depicted in Fig. 5. The q_e value (in mg g^{-1}) in this figure refers to the amount of amino acid (in mg) that has been adsorbed onto gram amount of $[\text{C}_8\text{MIM}]\text{-Fe}_3\text{O}_4$. Amino acids present both acid and base characteristics and thus changes in solution pH are expected to affect the adsorption mechanism and the extent in which Phe, Trp and Tyr are adsorbed onto the adsorbent surface.

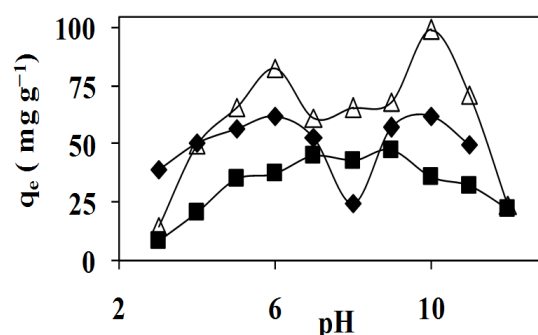


Fig. 5. Effect of pH of the sample solution on adsorptions of Phe, (■); Trp, (◆); and Tyr, (Δ). Experimental conditions: $[\text{C}_8\text{MIM}]\text{-Fe}_3\text{O}_4$ amount of 0.015 g , stirring time of 10 minutes, initial amino acid concentration of 100 mg L^{-1} .

In the present study, high adsorption capacity of nanoparticles for adsorption of Phe, Trp and Tyr was observed, respectively, at about pH 9.0, 6.0, 10.0. Results shown in Fig. 5 demonstrate that high loading for each amino acid occurs at two of these pH values after achieving the equilibrium condition; at pHs 6 and 10 for both Trp and Tyr; at pH 7.0 and 9.0 for Phe. At pH 3.0, Phe, Trp and Tyr molecules are predominantly positively charged (see Table 1 for pI values of Phe, Trp and Tyr) whereas the adsorbent surface is only slightly positively charged, so electrostatic repulsion is weak, and adsorption could occur strictly by hydrophobic interactions. At pHs, 9.0, 6.0 and 10.0, encompassing the pI, amino acids are in their zwitterionic forms. So, in pH 6.0, the electrostatic attraction between carboxylate anion and the positively-charged nanoparticles predominate. In pH 9.0 and 10.0, electrostatic attraction between protonated amino groups and the negatively-charged nanoparticles supports the adsorption process. At pH 8.0, where the nanoparticle surface is without charge, the hydrophobic attraction is the driving force for adsorption of three amino acids. At higher pH, the anionic form of amino acid predominates and an electrostatic repulsion is expected to be developed between both negatively-charged nanoparticles and anionic form of each amino acid. In addition, more adsorption of Tyr was observed at pH 10.0

than 6.0 that could be due to having hydroxyl group on its phenyl ring with a pK value of 10.07.

3.2.2. Effect of contact time

The effects of stirring (contact) time on the performance of [C₈MIM]-Fe₃O₄ for adsorbing of phenylalanine, tryptophan, and tyrosine was investigated. The [C₈MIM]-Fe₃O₄ amount of 0.015 g and the working pH for each amino acid solution (Phe, pH 7.0; Tyr, pH 10.0; and Trp, pH 6.0) were considered for performing this investigation. The initial amino acid concentration in each tested solution was 100 mg L⁻¹. Fig. 6 shows adsorption capacity of the adsorbent for three amino acids as a function of stirring time, ranging from 1.0 to 20.0 minutes. These data indicate that the adsorption process started immediately upon adding [C₈MIM]-Fe₃O₄ to each amino acid solution. Maximum adsorption for Phe, Tyr and Trp was observed after 15, 10 and 5 minutes, respectively.

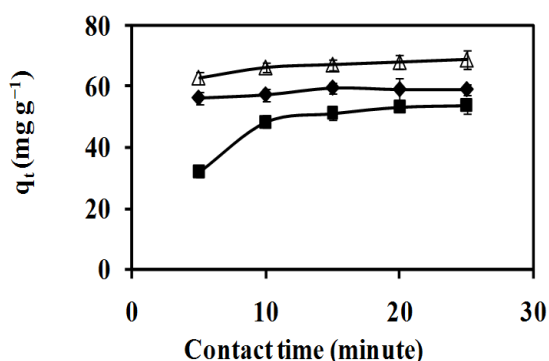


Fig. 6. Effect of stirring time on the adsorption of: Phe, (■); Trp, (◆); and Tyr, (Δ). Experimental conditions: [C₈MIM]-Fe₃O₄ amount of 0.015 g, initial amino acid concentration of 100 mg L⁻¹ at optimized pH value (Phe, pH 7.0; Tyr, pH 10.0; Trp, pH 6.0).

3.2.3. Effect of solution temperature

The effect of temperature on the adsorption of phenylalanine, tryptophan, and tyrosine by [C₈MIM]-Fe₃O₄ was investigated for each amino acid individually at their optimized pH and an initial amino acid concentration of 100 mg L⁻¹ with applying the optimized stirring time obtained for each amino acid (Phe, 15; Tyr, 10; Trp, 5 minutes). Fig. 7A shows the adsorption capacity

of the adsorbent for three amino acids as a function of temperature, ranging between 278 and 308 K. The results indicate that the solution temperature strongly affected the adsorption capacity of nanoparticles for adsorbing of Tyr and Trp. Adsorption capacity increases, with increasing temperature, indicates the endothermic nature of the three adsorption processes.

The plot of $\ln(q_e/C_e)$ versus $1/T$ is indicated in the inset of Fig. 7B; C_e is the equilibrium concentration of adsorbate. From the slope and intercept, the changes of enthalpy (ΔH) and entropy (ΔS) at 278-308 K could be determined. Table 2 shows the thermodynamic parameters for adsorption of phenylalanine, tryptophan, and tyrosine onto [C₈MIM]-Fe₃O₄ nanoparticles. The free energy of the adsorption processes for three amino acids, at the more temperatures, was negative indicating the spontaneity nature of the adsorption processes.

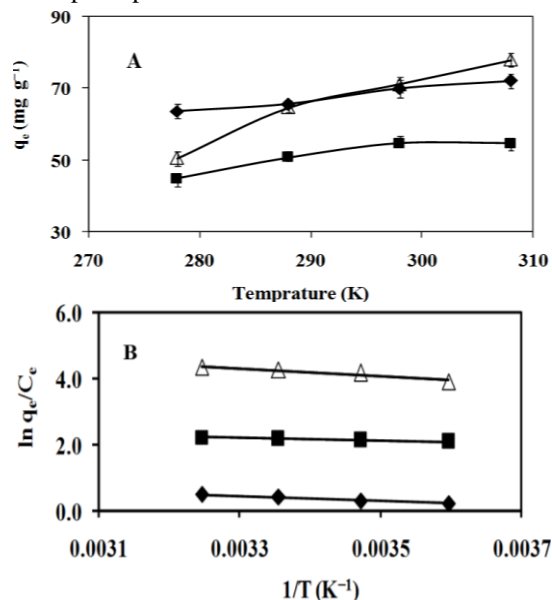


Fig. 7. (A) Effect of temperature on adsorption of: Phe, (■); Trp, (◆); and Tyr, (Δ). (B), the plots of $\ln(q_e/C_e)$ against $1/T$ for Phe, (■); Trp, (◆); and Tyr, (Δ). Experimental conditions: [C₈MIM]-Fe₃O₄ amount of 0.015 g, initial amino acid concentration of 100 mg L⁻¹ at optimized pH value (Phe, pH 7.0; Tyr, pH 10.0; Trp, pH 6.0), stirring time of (Phe, 15; Tyr, 10; Trp, 5 minutes).

Table 2. Thermodynamic parameters of amino acids-adsorption process onto [C₈MIM]-Fe₃O₄ nanoparticles. The error bars correspond to average deviations.

Amino acid	ΔS_0^T (J mol ⁻¹ K ⁻¹)	ΔH_0^T (kJ mol ⁻¹)	ΔG_0^T (kJ mol ⁻¹)			
			278 K	288 K	298 K	308 K
Tyr	68.89±0.5	9.99±0.1	-9.16±0.2	-9.50±0.1	-9.85±0.1	-11.22±0.2
Trp	25.59±0.8	6.63±0.2	-4.81±0.1	-7.36±0.2	-9.92±0.1	-12.48±0.3
Phe	29.96±1	3.54±0.1	-4.7±0.2	-5.09±0.2	-5.39±0.1	-5.69±0.1

The positive value of ΔH indicates that adsorption of phenylalanin, tryptophan and tyrosine onto $[\text{C}_8\text{MIM}]\text{-Fe}_3\text{O}_4$ is endothermic, i.e. higher adsorption can be obtained at higher temperatures. The ΔH includes two fractions, dehydration enthalpy, ΔH_d (endothermic); and adsorption affinity enthalpy, ΔH_a (exothermic); however, the endothermic effect of ΔH must be attributed to dehydration processes, i.e. ΔH_d predominates over ΔH_a so that the net enthalpy is positive in sign vice versa. Similarly, the entropy of adsorption is positive due to loss of water of the hydrated amino acids. Therefore, dehydration entropy, ΔS_d , predominates over adsorption affinity entropy, ΔS_a , and consequently the entropy of adsorption is positive for phenylalanin, tryptophan and tyrosine [38]. Since the free energy for hydrophobic interactions is lower than 20 kJ mol^{-1} (Table 2), the hydrophobic interaction for adsorption process in the studied temperature range is expected. The change in free energy for physisorption is between 20 and 0.0 kJ mol^{-1} , but for chemisorption is in the range of 80 to 400 kJ mol^{-1} . The values of ΔG obtained within the range of 20 and 0.0 kJ mol^{-1} , indicating that physisorption could be the dominating mechanism [39].

3.2.4. Adsorption isotherm modeling

Several isotherm models for evaluating the equilibrium adsorption, has discussed in literatures [40]. For evaluating the equilibrium adsorption, Freundlich and Dubinin-Radushkevich isotherm models were used. The Freundlich equation [41] is expressed in its linear form as follows:

$$\log q_e = \log K_F + \frac{1}{n} \log C_e \quad (2)$$

where K_F and n are the constants from the Freundlich equation representing the capacity of the adsorbent for the adsorbate and the reaction order, respectively. The reciprocal reaction order, $1/n$, is a function of the strength of adsorption. The Dubinin-Radushkevich isotherm model [42] is represented as:

$$q_e = q_D \exp\left(-B_D \left[RT \ln\left(1 + \frac{1}{C_e}\right)\right]^2\right) \quad (3)$$

where B_D is related to the free energy of sorption per mole of the sorbate as it migrates to the surface of the adsorbent from infinite distance in the solution and q_D is the Dubinin-Radushkevich isotherm constant related to the degree of sorbate sorption by the sorbent surface. The linear form of equation (4) is given as:

$$\ln q_e = \ln q_D - 2B_D RT \ln\left(1 + \frac{1}{C_e}\right) \quad (4)$$

The plots of $\ln q_e$ against $RT \ln(1+1/C_e)$, yields straight lines and indicates an apparent energy (E) of adsorption from the Dubinin-Radushkevich isotherm, which is calculated using equation (5)

$$E = 1/(2B_D)^{1/2} \quad (5)$$

Two different isotherm models, Freundlich and Dubinin-Radushkevich models, applied for isotherm adsorption analysis. Models fitted to equilibrium adsorption data of three amino acids were evaluated based on the values of the correlation coefficients (R^2) of their linear regression plots. The experimental data fitted with both models indicated that the adsorptions of three amino acids on $[\text{C}_8\text{MIM}]\text{-Fe}_3\text{O}_4$ nanoparticles are better described by Freundlich model. This in turn suggests that adsorption of amino acid occurs as heterogeneous onto the adsorbent surface. The resulting plots for Freundlich and Dubinin-Radushkevich model are shown in Fig. 8A and 8B. Table 3 summarizes the model constants and the correlation coefficient. Table 3 shows that the maximum adsorption capacity of nanoparticle for adsorption of Phe, Trp and Tyr are 0.22, 0.02 and $0.07 \text{ mmol amino acid per gram } [\text{C}_8\text{MIM}]\text{-Fe}_3\text{O}_4$, respectively.

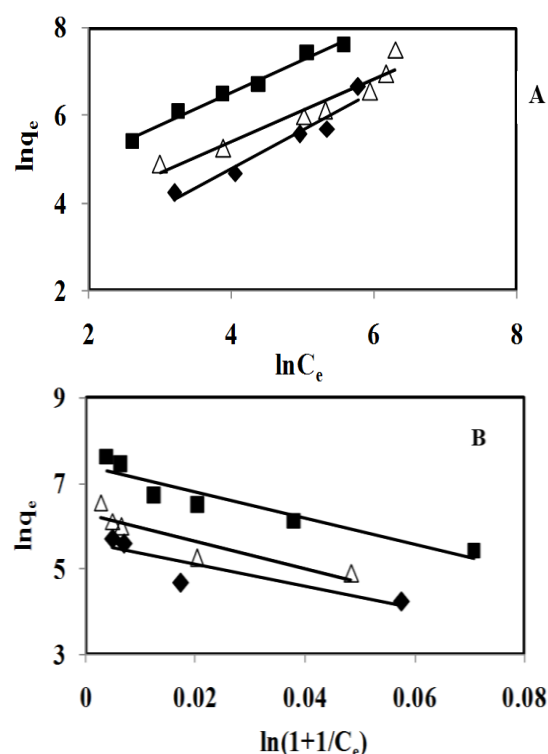


Fig. 8. (A), Freundlich isotherm plots; (B), Dubinin-Radushkevich for adsorption of: Phe, (■); Trp, (◆); and Tyr, (△) onto $[\text{C}_8\text{MIM}]\text{-Fe}_3\text{O}_4$ nanoparticles. Experimental conditions: $[\text{C}_8\text{MIM}]\text{-Fe}_3\text{O}_4$ amount of 0.015 g, at optimized pH value (Phe, pH 7.0; Tyr, pH 10.0; Trp, pH 6.0), stirring time of (Phe, 15; Tyr, 10; Trp, 5 minutes).

Table 3. Adsorption isotherm parameters for adsorption of Tyr, Trp and Phe onto [C₈MIM]-Fe₃O₄.

Amino acid	Dubinin – Radushkevich model			Freundlich model			
	Q _D (mg g ⁻¹)	B _D (mol ² kJ ⁻²)	R ²	E kJ mol ⁻¹	K _F (mg g ⁻¹)	n (g L ⁻¹)	R ²
Tyr	540.2	0.0065	0.830	11.87	12.74	1.40	0.921
Trp	272.0	0.0052	0.720	18.43	3.55	1.14	0.940
Phe	1639.2	0.0061	0.884	13.08	35.62	1.35	0.982

Table 4. Comparisons of the proposed adsorbent and other adsorbent for the adsorption of Phe, Trp and Tyr.

Adsorbent	Amino acid	K _F (mmol g ⁻¹)	n	Equilibrium time	Reference
carboxymethyl-β-cyclodextrin bonded Fe ₃ O ₄ /SiO ₂ core-shell nanoparticles	L-Phe	0.027	1.130	Less than 24 h	Gosh et al. (2011)
	L-Trp	0.151	3.557	Less than 24 h	
	L-Tyr	0.018	1.009	Less than 24 h	
	L-Phe	0.220	1.350	15 min	
[C ₈ MIM]-Fe ₃ O ₄ nanoparticles	L-Trp	0.02	1.140	10 min	This work
	L-Tyr	0.07	1.400	5 min	

These results reveal that higher adsorption of three amino acids are possible with [C₈MIM]-Fe₃O₄ nanoparticles. Adsorption of amino acids on the surface of [C₈MIM]-Fe₃O₄ nanoparticles is concluded to be attributed to the surface electrostatic and hydrophobic interactions between amino acids and [C₈MIM]-Fe₃O₄ nanoparticles. It should be mentioned that the amino acid adsorption process is affected by the chemical properties of the tested amino acids and adsorbent. The difference in adsorption capacity of nanoparticle for adsorption of Phe, Trp and Tyr may be attributed to their chemical structures and physical properties, particularly the difference in the size and hydrophobicity of amino acids molecules (Table 1). Maximum adsorption capacity of [C₈MIM]-Fe₃O₄ nanoparticles was observed for Phe which have the smallest size and the most hydrophobicity index among the three amino acids. However, size of Trp molecule is bigger than that of Tyr, but their hydrophobicity is same. Therefore adsorption capacity of [C₈MIM]-Fe₃O₄ nanoparticles for Tyr is more than Trp [43]. The maximum adsorption capacity of nanoparticle for Phe, Trp and Tyr was occurred due to their higher negative charges that effectively interact with the positive charges of [C₈MIM]-Fe₃O₄ nanoparticles. It is noticeable that the lower adsorption capacity for Trp could be explained due to large size of Trp and a weak hydrophobic interactions between Trp and [C₈MIM]-Fe₃O₄ nanoparticles.

Table 4 presents a comparison between the proposed adsorbent and another adsorbent reported in literature for adsorption of L-Phe, L-Trp and L-Tyr. As it is shown in this table, the adsorption capacity (obtained based on the Freundlich model) of the fabricated adsorbent is higher for L-Phe (0.220 versus 0.027 mmole per gram) and L-Tyr (0.07 versus 0.018 mmole per

gram). However, the uptake of L-Trp by the developed adsorbent is worse. The short equilibrium time (≤ 15 minutes versus 24 hours) for the adsorption of amino acids by the developed adsorbent is significantly higher than the other adsorbent which could be considered as one of the highlighted advantages of our presented adsorbent.

3.2.5. Adsorption kinetic modeling

Several models are available to study the adsorption mechanism and describe the corresponding experimental data. The most commonly models used are the pseudo-first-order and pseudo-second-order reaction rate equations developed by Ho and McKay [44].

Pseudo-first-order equation:

$$\log(q_e - q_t) = \log q_e - k_1 t \quad (6)$$

Pseudo-second-order equation:

$$\frac{t}{q_t} = \frac{1}{k_2 q_e^2} + \frac{t}{q_e} \quad (7)$$

where k₁ and k₂ are the adsorption rate constants of first and second kinetic models, q_t is adsorption capacity at time t, q_e is adsorption capacity at equilibrium condition.

In order to investigate the mechanisms of metal adsorption process, the linearized equations of pseudo-first-order and pseudo-second-order kinetic models were applied. Table 5 gives a summary of the models and the corresponding constants along with the correlation coefficients for the linear regression plots of the three tested amino acids. Higher values of R² were obtained for pseudo-second order model indicating that the adsorption rates for Phe, Trp and Tyr can be more appropriately described using the pseudo-second-order rate.

Intra-particle diffusion is a transport process involving movement of species from the bulk of

Table 5. Adsorption kinetic constants for tyrosin, tryptophan and phenylalanin onto [C₈MIM]-Fe₃O₄ nanoparticles.

Amino acid	Pseudo-first-order model			Pseudo-second-order model			Intra-particle diffusion		
	k _i (min ⁻¹)	q _e (mg g ⁻¹)	R ²	k ₂ (g mg ⁻¹ min ⁻¹)	q _e (mgg ⁻¹)	R ²	k _i (g mg ⁻¹ min ⁻¹)	C (mg g ⁻¹)	R ²
Tyr	0.13	10.38	0.987	0.024	71.4	0.999	2.65	57.5	0.941
Trp	0.11	4.9	0.947	0.051	62.5	0.999	1.13	53.9	0.971
Phe	0.24	69.7	0.981	0.0036	66.7	0.991	2.35	42.5	0.916

the solution to the solid phase. The intra-particle kinetic model is expressed by

$$Q_t = k_i t^{1/2} + C$$

where k_i is an intra-particle diffusion rate constant and Q_t is amount of adsorbate adsorbed at time t. Initially, the external surface adsorption, which is faster, is completed, and then, the intra-particle diffusion is attained. A plot of the amount of sorbate adsorbed, q_t (mg g⁻¹) vs. the square root of the time, gives the rate constant (slope of the plot) and the intercept is proportional to the boundary layer thickness. The correlation coefficient (R²) value of the model indicates the possibility of intra-particle diffusion (Table 5) for the amino acids adsorbed onto magnetic nanoparticles. Since the plots do not pass through the origin, the boundary layer diffusion may be involved in rate limiting step. The first linear portion corresponds to the gradual adsorption stage where the intra-particle diffusion is the rate-limiting step. The second linear portion can be considered as the final equilibrium stage where intra-particle diffusion begins to slow down because of the extremely low amino acid concentration in the solution and the amino acid molecules occupied all the active sites of the nanoparticle [45].

3.2.6. Desorption and reusability studies

For potential applications, the regeneration and reusability of an adsorbent are important factors to be reported. Possible desorption of phenylalanine, tryptophan, and tyrosine (20 mg L⁻¹) was tested by sodium chloride (1.0 and 2.0 mol L⁻¹), sodium hydroxide (1.0 and 2.0 mol L⁻¹) and mixed of sodium chloride (1.0 mol L⁻¹) and sodium hydroxide solutions (1 mol L⁻¹). The desorption ratio, defined as the ratio of the amount of amino acid in the desorption medium to the amount of amino acid initially adsorbed on [C₈MIM]-Fe₃O₄ nanoparticles, was calculated. The results showed that the desorption ratios were about 95%, 93% and 91% for phenylalanine, tryptophan, and tyrosine, respectively. The study revealed that the adsorbed phenylalanine and tyrosine could be completely desorbed in the presence of 1.0 and 2.0 mol L⁻¹ NaOH, respectively. The adsorbed tryptophan could be completely desorbed in the presence of mixture of NaCl (1.0 mol L⁻¹) and NaOH (1.0 mol L⁻¹). The

results showed that 91-95% of amino acids could be desorbed and recovered by 10 mL of desorption solution (1.0 mol L⁻¹) in 20 minutes, when amino acid concentration of 5×10⁻⁴ mol L⁻¹ was already adsorbed on 0.015 g [C₈MIM]-Fe₃O₄ nanoparticles. Addition of desorbing solution in three consecutive desorption process completed the desorption process.

The reusability of the adsorbents in several successive separation processes was tested and the result showed that the [C₈MIM]-Fe₃O₄ nanoparticles can be reused for three times without significant reduction in its removal capacity.

4. CONCLUSION

The [C₈MIM]-Fe₃O₄ nanoparticles were quite efficient as magnetic nano-adsorbents for fast adsorption of Phe, Trp and Tyr from aqueous solutions. The time required to achieve the adsorption equilibrium was 15, 10, 5 minutes for Phe, Trp and Tyr. The adsorption of the tested amino acids on the surface of [C₈MIM]-Fe₃O₄ nanoparticles was concluded to be attributed to the surface electrostatic and/or hydrophobic interactions between amino acids and [C₈MIM]-Fe₃O₄ nanoparticles. The experimental data indicated that the adsorptions of Phe, Trp and Tyr on [C₈MIM]-Fe₃O₄ nanoparticles are better described by the Freundlich. The changes of enthalpy (ΔH) were determined to be 3.54, 6.63 and 9.99 kJ mol⁻¹ for Phe, Trp and Tyr in the same order. Kinetic data were appropriately fitted to the pseudo-second order adsorption rates. The adsorbed phenylalanine and tyrosine could be completely desorbed in the presence of 1.0, 2.0 mol L⁻¹ NaOH, respectively. The adsorbed tryptophan could be completely desorbed in the presence of a mixture of NaCl (1.0 mol L⁻¹) and NaOH (1.0 mol L⁻¹). The reusability of [C₈MIM]-Fe₃O₄ was found to be for three times.

ACKNOWLEDGMENTS

The authors wish to acknowledge the support of this work by Payame Noor University. I would like to thank E. Seyghalani Talab of Payame Noor University and Prof. G. Absalan of Department of Chemistry at Shiraz University for their technical assistance.

REFERENCES

- [1] J.E. Krohn and M. Tsapatsis, Amino acid adsorption on zeolite, *Langmuir* 21 (2005) 8743-8750.
- [2] A.J. O'Connor, A. Hokura, J.M. Kisler, S. Shimazu, G.W. Stevens and Y. Komatsu, Amino acid adsorption onto mesoporous silica molecular sieves, *Sep. Purif. Technol.* 48 (2006) 197-201.
- [3] F. Sanda and T. Endo, Syntheses of functions polymers based on amino acids, *Macromol. Chem. Phys.* 200 (1999) 2651-2661.
- [4] S.L. Bourke and J. Kohn, Polymers derived from the amino acid L-tyrosine: polycarbonates, polyarylates and copolymers with poly(ethylene glycol), *Adv. Drug Delivery Rev.* 55 (2003) 447-466.
- [5] W. Notz, F. Tanaka and C.F. Barbas, Enamine-Based Organocatalysis with Proline and Diamines: The Development of Direct Catalytic Asymmetric Aldol, Mannich, Michael, and Diels–Alder Reactions, *Acc. Chem. Res.* 37 (2004) 580-591.
- [6] J. Goscińska, A. Olejnik and R. Pietrzak, Adsorption of L-phenylalanine onto mesoporous silica, *Mater. Chem. Phys.* 142 (2013) 586-593.
- [7] C.C.O. Alves, A.S. Franca and L.S. Oliveira, Removal of phenylalanine from aqueous solutions with thermo-chemically modified corn cobs as adsorbents, *LWT - Food Sci. Technol.* 51 (2013) 1-8.
- [8] M. Ikeda and R. Katsumata, Hyperproduction of tryptophan by *Corynebacterium glutamicum* with the modified pentose phosphate pathway, *Appl. Environ. Microbiol.* 65 (1999) 2497-2502.
- [9] Y.M. Chao and T.M. Liang, A feasibility study of industrial wastewater recovery using electro dialysis reversal, *Desalination*, 221 (2008) 433-439.
- [10] T. Oshima, R. Saisho, K. Ohe, Y. Baba and K. Ohto, Adsorption of amino acid derivatives on calixarene carboxylic acid impregnated resins, *React. Funct. Polym.* 69 (2009) 105-110.
- [11] G. Absalan, M. Akhond and L. Shekhan, Partitioning of acidic, basic and neutral amino acids into imidazolium-based ionic liquids, *Amino Acids* 39 (2010) 167-174.
- [12] Y. Wang, C. Shi, Q. Gan and Y. Dai, Separation of amino acids by polymeric reversed micelle extraction, *Sep. Purif. Technol.* 35 (2004) 1-9.
- [13] Y. Xie, K.J. Jing and Y. Lu, Kinetics, equilibrium and thermodynamic studies of L-tryptophan adsorption using a cation exchange resin, *Chem. Eng. J.* 171 (2011) 1227-123.
- [14] C. Namasivayam, M. Dineshkumar, K. Selvi, R.A. Begum, T. Vanathi and R.T. Yamuna, 'Waste' coir pith-a potential biomass for the treatment of dyeing wastewaters, *Biomass Bioenergy* 21 (2001) 477-483.
- [15] J. Orthman, H.Y. Zhu and G.Q. Lu, Use of anion clay hydrotalcite to remove coloured organics from aqueous solutions, *Sep. Sci. Technol.* 31 (2003) 53-59.
- [16] S.J.T. Pollard, G.D. Fowler, C. J. Sollars and R. Perry, Low-cost adsorbents for waste and wastewater treatment: A review, *Sci. Total Environ.* 116 (1992) 31-52.
- [17] J. Qi, L. Zhi, Y. Guo and H. Xu, Adsorption of phenolic compounds on micro- and mesoporous rice husk-based active carbons, *Mater. Chem. Phys.* 87 (2004) 96-101.
- [18] C. Tizaoui and M.J. Slater, The design of an industrial waste-water treatment process using adsorbed ozone on silica gel, *Process Saf. Environ.* 81 (2003) 107-113.
- [19] K. Knaebel, For your next separation consider adsorption, *Chem. Eng.* 102 (1995) 92-100.
- [20] J. Fei-peng, F. Zhao-di, S. Li and C. Xiao-qing, Removal of phenylalanine from water with calcined CuZnAlCO_3 layered double hydroxides, *Trans. Nonferrous Met. Soc. China* 22 (2012) 476-482.
- [21] G. Keller, Adsorption: building upon a solid foundation, *Chem. Eng. Prog.* 91 (1995) 56-67.
- [22] G. Absalan and M. Ghaemi, Investigating the parameters affecting the adsorption of amino acids onto AgCl nanoparticles with different surface charges. *Amino Acids* 43 (2012) 1955-1967.
- [23] Z.Z. Yang, Y.N. Zhao and L.N. He, CO_2 chemistry: task-specific ionic liquids for CO_2 capture/activation and subsequent conversion, *RSC Adv.* 1 (2011) 545-567.
- [24] G.T. Wei, Z. Yang and C. J. Chen, Room temperature ionic liquid as a novel medium for liquid/liquid extraction of metal ions, *Anal. Chim. Acta* 488 (2003) 183-192.
- [25] S. Kamran, H. Tavallali and A. Azad, Fast Removal of Reactive Red 141 and Reactive Yellow 81 from Aqueous Solution by Fe_3O_4 Magnetic Nanoparticles Modified with 1-Octyl-3-methylimidazolium bromide, *Iran. J. Anal. Chem.* 1 (2014) 78-86.
- [26] M.D. Farahani and F. Shemirani, Supported hydrophobic ionic liquid on magnetic nanoparticles as a new sorbent for separation

- and preconcentration of lead and cadmium in milk and water samples, *Microchim. Acta* 179 (2012) 219-226.
- [27] Q. Zhang, F. Yang, F. Tang, K. Zeng, K. Wu, Q. Cai and S. Yao, Ionic liquid-coated Fe₃O₄ magnetic nanoparticles as an adsorbent of mixed hemimicelles solid-phase extraction for preconcentration of polycyclic aromatic hydrocarbons in environmental samples, *Analyst* 135 (2010) 2426-2433.
- [28] D. Long, R. Zhang, W. Qiao, L. Zhang, X. Liang and L. Ling, Biomolecular adsorption behavior on spherical carbon aerogels with various mesopore sizes, *J. Colloid Interf. Sci.* 331 (2009) 40-46.
- [29] P. Bonhote, A. P. Dias, N. Papageorgion, K. Kalyanasundaran and M. Gratzel, Highly conductive ambient-temperature molten salts, *Inorg. Chem.* 35 (1996) 1168-1178.
- [30] D.K. Kim, Y. Zhang, W. Voit, K.V. Rao and M. Muhammed, Synthesis and characterization of surfactant-coated superparamagnetic monodispersed iron oxide nanoparticles, *J. Magn. Magn. Mater.* 225 (2001) 30-36.
- [31] G. Absalan, S. Kamran, M. Asadi, L. Sheikhan and M. D. Goltz, Removal of reactive red-120 and 4-(2-pyridylazo) resorcinol from aqueous samples by Fe₃O₄ magnetic nanoparticles using ionic liquid as modifier, *J. Hazard. Mater.* 192 (2011) 476-484.
- [32] S.I. Park, J.H. Kim, J.H. Lim and C.O. Kim, Surface-modified magnetic nanoparticles with lecithin for applications in biomedicine, *Curr. Appl. Phys.* 8 (2008) 706-709.
- [33] D. Faivre and P. Zuddas, An integrated approach for determining the origin of magnetite nanoparticles, *Earth Planet. Sci. Lett.* 243 (2006) 53-60.
- [34] R.D. Waldron, Infrared spectra of ferrites, *Phys. Rev.* 99 (1955) 1727-1735.
- [35] K. Can, M. Ozmen and M. Ersoz, Immobilization of albumin on aminosilane modified superparamagnetic magnetite nanoparticles and its characterization, *Colloids Surf. B Biointerfaces* 71 (2009) 154-159.
- [36] M.T. Uddin, M.A. Islam, S. Mahmud and M. Rukanuzzaman, Adsorptive of removal of methylene blue by tea waste, *J. Hazard. Mater.* 164 (2009) 53-60.
- [37] J. Li, X. Zhao, Y. Shi, Y. Cai, S. Mou and G. Jiang, Mixed hemimicelles solid-phase extraction based on cetyltrimethylammonium bromide-coated nano-magnets Fe₃O₄ for the determination of chlorophenols in environmental water samples coupled with liquid chromatography/spectrophotometry detection, *J. Chromat. A* 1180 (2008) 24-31.
- [38] X.P. Geng, M.R. Zheng, B.H. Wang, Z.M. Lei and X.D. Geng, Fractions of thermodynamic functions for native lysozyme adsorption onto moderately hydrophobic surface, *J. Therm. Anal. Calorim.* 93 (2008) 503-508.
- [39] S. Kamran, M. Asadi and G. Absalan, Adsorption of acidic, basic, and neutral proteins from aqueous samples using Fe₃O₄ magnetic nanoparticles modified with an ionic liquid, *Microchim. Acta* 108 (2013) 41-48.
- [40] G. Limousin, P. Gaudet, L. Charlet, S. Szenknect, V. Barthés and M. Krimissa, Sorption isotherms: A review on physical bases, modeling and measurement, *Appl. Geochem.* 22 (2007) 249-275.
- [41] D.A. Uygun, A.A. Karagözler, S. Akgöl and A. Denizli, Magnetic hydrophobic affinity nanobeads for lysozyme separation, *Mater. Sci. Eng. C* 29 (2009) 2165-2173.
- [42] M. Horsfall, A.I. Spiff and A.A. Abia, Studies on the influence of mercaptoacetic acid (MAA) modification of cassava (*Manihot sculenta* cranz) waste Biomass on the adsorption of Cu²⁺ and Cd²⁺ from aqueous solution, *Bull. Korean Chem. Soc.* 25 (2004) 969-976.
- [43] S. Ghosh, A.Z. M. Badruddoza, M.S. Uddin and K. Hidajat, Adsorption of chiral aromatic amino acids onto carboxymethyl- β -cyclodextrin bonded Fe₃O₄/SiO₂ core-shell nanoparticles, *J. Colloid Interf. Sci.* 354 (2011) 483-492.
- [44] Y.S. Ho and G. McKay, Pseudo-second-order model for sorption processes, *Process Biochem.* 34 (1999) 45-465.
- [45] K.A.G. Gusmão, L.V.A. Gurgel, T.M.S. Melo and L.F. Gil, Application of succinylated sugarcane bagasse as adsorbent to remove methylene blue and gentian violet from aqueous solutions-Kinetic and equilibrium studies, *Dyes Pigm.* 92 (2012) 967-974.